Ship resistance analysis using CFD simulations in Flow-3D

S Deshpande*, P Sundsbø, S Das

Department of Building, Energy and Material Technology,
UiT, The Arctic University of Norway, 8514 Narvik, Norway

ABSTRACT

While designing the power requirements of a ship, the most important factor to be considered is the ship resistance, or the sea drag forces acting on the ship. It is important to have an estimate of the ship resistance while designing the propulsion system since the power required to overcome the sea drag forces contribute to 'losses' in the propulsion system. There are three main methods to calculate ship resistance: Statistical methods like the Holtrop-Mennen (HM) method, numerical analysis or CFD (Computational Fluid Dynamics) simulations, and model testing, i.e. scaled model tests in towing tanks. At the start of the design stage, when only basic ship parameters are available, only statistical models like the HM method can be used. Numerical analysis/ CFD simulations and model tests can be performed only when the complete 3D design of the ship is completed. The present paper aims at predicting the calm water ship resistance using CFD simulations, using the Flow-3D software package. A case study of a roll-on/roll-off passenger (RoPax) ferry was investigated. Ship resistance was calculated at various ship speeds. Since the mesh affects the results in any CFD simulation, multiple meshes were used to check the mesh sensitivity. The results from the simulations were compared with the estimate from the HM method. The results from simulations agreed well with the HM method for low ship speeds. The difference in the results was considerably high compared to the HM method for higher ship speeds. The capability of Flow-3D to perform ship resistance analysis was demonstrated.

1. INTRODUCTION

It is important to confirm the performance characteristics of a ship before construction because of the complexities and high costs involved in construction [1]. Ship resistance is one of the performance characteristics and is defined as the force required to overcome the hydrodynamic and air resistance that works against its movement. The components of the hydrodynamic resistance include frictional resistance, viscous pressure resistance and the wave resistance. Ship resistance calculations for non-high-speed models usually neglect the air resistance. This is attributed to the fact that the air drag of the ship's superstructure constitutes only a small percentage (2-6%) of the total ship resistance depending on the type of the ship [2].

Ship resistance is also important while calculating the power requirement for propulsion [3]. Minimizing the ship resistance results in reduced power requirement for the ship. A lower value of ship resistance thus amounts to lower fuel consumption, which is economically and environmentally beneficial.

*Corresponding Author: sujay.r.deshpande@uit.no

Shipping constitutes almost 90% of global trade. There is a significant environmental impact of such high volumes of shipping and it can be considered as a major contributor to climate change [4]. It is an aim for ship designers to minimize ship resistance. Design modifications based on analysis of ship resistance are a part of the ship design process.

The HM method is based on regression analysis of existing full-scale data. It is an extremely useful tool to estimate ship resistance in early stages of the ship design process. However, it is necessary to understand that statistical methods give only a rough estimate and might have considerable variations from the actual values of ship resistance [5].

Model tests are performed in towing tanks to find the ship resistance once the design is finalized. Prototyping of a scaled model and testing in towing tanks are expensive and time-consuming procedures. In addition, the results from the model tests have to be scaled to the actual size of the ship, a process involving certain uncertainties [6].

CFD analysis is becoming the preferred method over model tests for calculating ship resistance due to availability of powerful computational resources and advancements in the field of CFD [7].

This paper presents a procedure for CFD simulations to calculate the calm water ship resistance with a case study of a roll-on/roll-off passenger (RoPax) ferry. The software used is Flow-3D. Simulations were carried out at different ship speeds from the average operating speed of 10 knots to the maximum operating speed of 24 knots as provided by the ship designers. Mesh sensitivity was evaluated by simulations with different meshes. Results from all the simulations were compared to the calculations by the HM method.

It was observed that the results for ship resistance from the CFD simulations confirm well with the calculations with the HM method at lower ship speeds. At higher ship speeds, there is a considerable deviation between the two methods.

It is also shown that Flow-3D is suitable for hydrodynamic simulations with a free surface interface and can be used for running ship resistance simulations.

2. HOLTROP-MENNEN METHOD

An approximate power prediction method' written by J. Holtrop and G.G.J. Mennen in 1982 proposed a method to predict ship resistance and power requirements at an early design stage. The method uses regression analysis of data from a large number of model tests carried out at the Netherlands Ship Model Basin [5]. The HM method has proved to be a handy tool for estimating ship resistance in the early design stages when the number of known parameters were limited [8]. CFD analysis on the other hand, is performed when the hull design is ready, and to check for minor design modifications depending on the results. The difference in the objectives of both of these methods makes it unlikely that the HM method is completely replaced with CFD.

Deviation from the actual values of ship resistance is expected while using the HM method owing to it being a statistical method based on previous ship designs. It is thus interesting to know how the HM method performs compared to CFD simulations.

If the basic design parameters of the ship are known, using the HM method is straightforward. Holtrop and Mennen describe the process of using this method in detail in their article 'An approximate power prediction method [5]. Due to the confidentiality, details regarding the calculations involved in the HM method are not divulged and the results are presented directly.

3. COMPUTATIONAL FLUID DYNAMICS

Analysis using CFD involves solving the governing equations of fluid flow numerically. The three governing equations of fluid flow are the continuity equation or the mass conservation equation, the momentum conservation equation or the Navier-Stokes equations, and the energy conservation equation. Every CFD code solves the mass and momentum conservation equations in the background as these form the basis of any fluid calculations.

For incompressible flows, the mass conservation or the continuity equation is given as shown in Equation (1):

$$\frac{\partial u}{\partial x} + \frac{\partial v}{\partial y} + \frac{\partial w}{\partial z} = 0 \tag{1}$$

where u, v, and w are the fluid velocities in the x, y, and z directions, respectively.

The Navier-Stokes (N-S) or momentum equations are a form of Newton's second law to describe fluid motion. The momentum conservation equations for three-dimensional flows are shown in Equations (2-4):

$$\rho \left(\frac{\partial u}{\partial t} + u\frac{\partial u}{\partial x} + v\frac{\partial u}{\partial y} + w\frac{\partial u}{\partial z} \right) = -\frac{\partial p}{\partial x} + \rho g_x + \mu \left(\frac{\partial^2 u}{\partial x^2} + \frac{\partial^2 u}{\partial y^2} + \frac{\partial^2 u}{\partial z^2} \right) \tag{2}$$

$$\rho \left(\frac{\partial v}{\partial t} + u\frac{\partial v}{\partial x} + v\frac{\partial v}{\partial y} + w\frac{\partial v}{\partial z} \right) = -\frac{\partial p}{\partial y} + \rho g_y + \mu \left(\frac{\partial^2 v}{\partial x^2} + \frac{\partial^2 v}{\partial y^2} + \frac{\partial^2 v}{\partial z^2} \right) \tag{3}$$

$$\rho \left(\frac{\partial u}{\partial t} + u\frac{\partial w}{\partial x} + v\frac{\partial w}{\partial y} + w\frac{\partial w}{\partial z} \right) = -\frac{\partial p}{\partial z} + \rho g_z + \mu \left(\frac{\partial^2 w}{\partial x^2} + \frac{\partial^2 w}{\partial y^2} + \frac{\partial^2 w}{\partial z^2} \right) \tag{3}$$

where ρ is the density of the fluid, p is the pressure, g is acceleration due to gravity, μ is the fluid viscosity and u, v, and w are the fluid velocities in the x, y, and z directions respectively. The left-hand side of the N-S equations are the acceleration equations whereas the right hand side includes forces, gravity and pressure [9].

Flow-3D, which is a commercial CFD package was used in this study. Flow-3D uses the TruVOF (True Volume Of Fluid) method based on the SOLA (SOLution Algorithm) algorithm developed by Hirth and Nicolas described in their 1981 article 'Volume of fluid (VOF) method for the dynamics of free boundaries' [10]. Flow-3D is written in Fortran 90. Fortran is a widely used computing language by the scientific community for mathematical and scientific computing [11].

4. SIMPLIFICATION OF THE SHIP GEOMETRY

The detailed 3D ship model available from the ship designers was simplified by taking away the equipment, side railings and other details of the ship geometry that were not influential for this study as shown in Figure 1. This was done taking into consideration computational limitations. The changes have limited to no effect to the ship resistance study since the hull form and other details of the ship geometry under the water surface level was not changed.
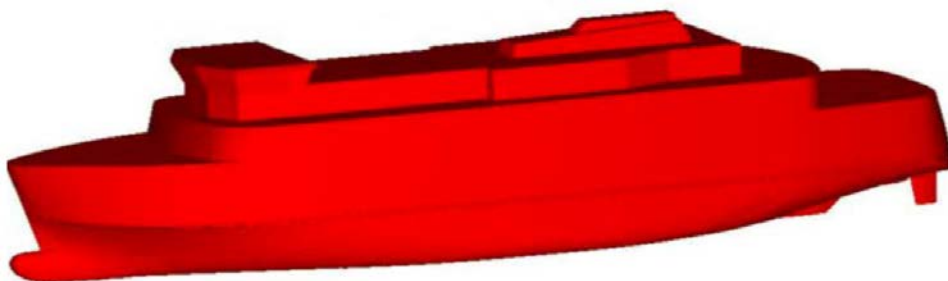
Figure 1: Simplified ship geometry

5. MESHING

5.1. Free gridding in Flow-3D

Flow-3D implements 'free gridding' using the Fractional Area Volume Obstacle Representation - FAVOR. Simple rectangular construction of grids in Flow-3D makes the mesh extremely easy to generate. This gridding technique is unique to Flow-3D and the numerical accuracy is not sacrificed when selecting FAVOR over a body-fitted coordinate gridding method [12].

5.2. Mesh

The mesh requires enough space between the ship and fluid inlet and the domain boundary and the sides of the ship. The fluid domain at the aft of the ship is for avoiding restrictions of flow. To avoid shallow water effects that might lead to higher values of ship resistance, the fluid depth was kept approximately as twice the length of the hull. A finer mesh was constructed at the interface of the ship geometry and the fluid. Since the motion in calm waters involves only the waves formed due to ship-sea interaction, which have a relatively low amplitude, the fine mesh is required only up to a small height over the fluid surface. The mesh is shown in Figure 2.
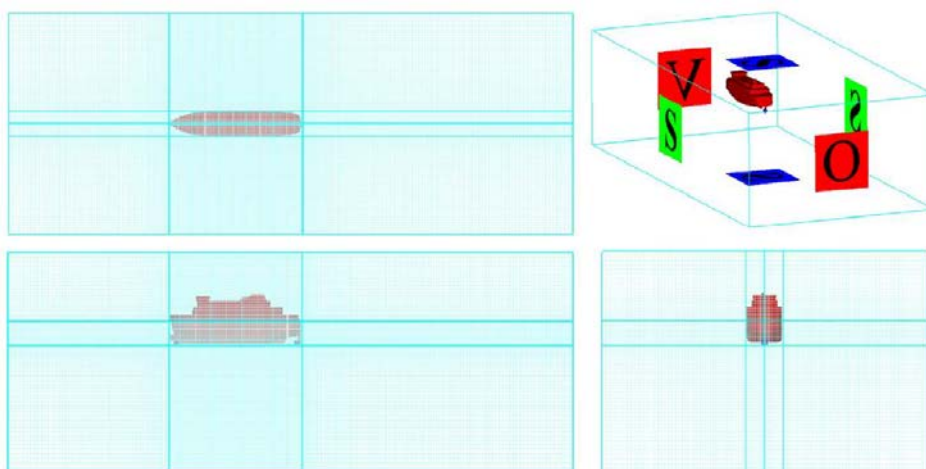

Figure 2: Meshing: 'Free gridding' with FAVOR method in Flow-3D

5.3. Boundary conditions
The boundary conditions used for the case are shown in Figure 2. 'V' represents a velocity inlet where the inlet velocity of the fluid corresponds to the ship speed in m/s. 'O' represents outlet. 'S' represents a symmetry boundary type used on the left, right, top and bottom boundaries. Additional shallow water effects are avoided by using symmetry for the bottom boundary.

5.4. Fluid Height
In Flow-3D, fluid height can be provided if fluid enters through only a part of the boundary while using a velocity input boundary condition. The fluid height was adjusted to match the waterline of the ship.

Three different mesh sizes were used to study the mesh sensitivity.

Table 1: Mesh variations

Mesh	Outer mesh cell size (m)	Inner mesh cell size (m)
Mesh 1	1.00	0.500
Mesh 2	0.75	0.375
Mesh 3	0.50	0.250

6. SIMULATION SETTINGS

6.1. General settings
The mass of the ship and the location of the center of gravity were given as inputs. Other input variables include acceleration due to gravity, $g = 9.81 \ m/s$, density of water, $\rho_{water} = 1027 \ kg/m^3$, and dynamic viscosity of water, $\mu = 0.00148 \ pas$. The simulations were run until the stability was confirmed.

6.2. Turbulence model
The governing equations of fluid flow are usually simplified by using turbulence models, without which the computing time would be substantially large [13]. The simulations used RANS (Reynolds Averaged Navier Stokes) k-ε model, that is typical for external flows with complex geometry. The parameters k and ε are calculated by solving the transport equations for each of these quantities along with the equations describing the mean flow [14].

6.3. General Moving Objects in Flow-3D
A general moving object is a rigid body with six degrees of freedom, of which any of the rotations or the translations can be either constrained by the user or dynamically coupled with the fluid [15]. Flow-3D includes the option of using the General Moving Objects (GMO) model in which the 'implicit' option was selected. The motion of the ship was constrained to allow pitching and movement along the axis perpendicular to the water surface.

6.4. Moment of inertia

The General Moving Objects model in Flow-3D requires inputs for the moment of inertia tensor about the mass center in the body system. Usually, this is calculated by the software itself with the data from the geometry and mass. However, the mass distribution of the on-board contents and the internal architecture affect the mass center and moment of inertia compared to a simplified solid model. Thus, the values of the moment of inertia tensors about the mass center provided by the ship designers were used.

For each mesh mentioned in Table 1, simulations were carried out at ship speeds mentioned in Table 2, starting with the average operating speed of 10 knots to the maximum operating speed of 24 knots.

Table 2: Ship speeds

Case no.	Ship speed (knots)	Ship speed (m/s)
Case 1	10	5.14
Case 2	15	7.72
Case 3	20	10.29
Case 4	24	12.35

7. RESULTS AND DISCUSSION

The results of the ship resistance values from the Holtrop-Mennen method and all the simulations are presented in Table 3 and Figure 4. Results show that the ship resistance increases considerably with increase in the ship speed.

The generated wave pattern due to the ship-sea interaction in case of the simulation for ship speed of 20 knots and mesh 1 is shown in Figure 3. The velocity profile on the fluid surface is not consequential for this study and hence is not mentioned.
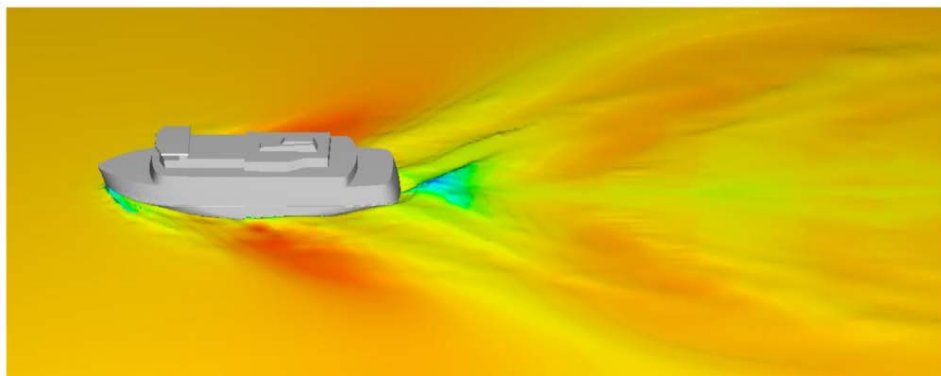

Figure 3: Wave pattern at sea surface at 20 knots (10.29 m/s) for mesh 1

Values of ship resistance from the simulations confirm well with the calculations from the HM method for low ship speeds. However, for higher ship speeds, the simulations show a considerable deviation from the HM method.

Table 3: Ship resistance at various ship speeds

Ship speed (knots)	Mesh 1 (kN)	Mesh 2 (kN)	Mesh 3 (kN)	Holtrop-Mennen (kN)
10	53.2	52.7	49.7	51.7
15	214.5	205.4	196.1	152.3
20	677.8	636.6	593.5	383.6
24	1170.3	1097.9	1010.1	685.4

Despite the deviation, the trends of the ship resistance with respect to ship speed from the simulations and the HM method are similar as shown in Figure 4. The increase in the ship resistance with the increase in ship speed is non-linear. It increases steeply with the increase in ship speed. This is a result from the contribution of higher 'wave making and wave breaking resistance' at higher ship speeds. This study does not include the individual contributions from various components of the total ship resistance, but the reason for the increasing trend of ship resistance at higher ship speeds is well known in the ship design industry.

The ship resistance, when the air resistance is neglected, is the sum of the total hull resistance including frictional or viscous resistance, and the wave making and wave breaking resistance. The wave making and wave breaking resistance increase rapidly with increase in ship speed as compared to the total hull resistance. The increase in wave making and wave breaking resistance is much higher than the increase in frictional or viscous resistance [16]. At higher speeds, the waves generated as a result of the ship motion are higher. A greater amount of energy is spent in the generation of these high waves. The steep rise in the ship resistance at higher ship speeds is on account of this energy loss [16].
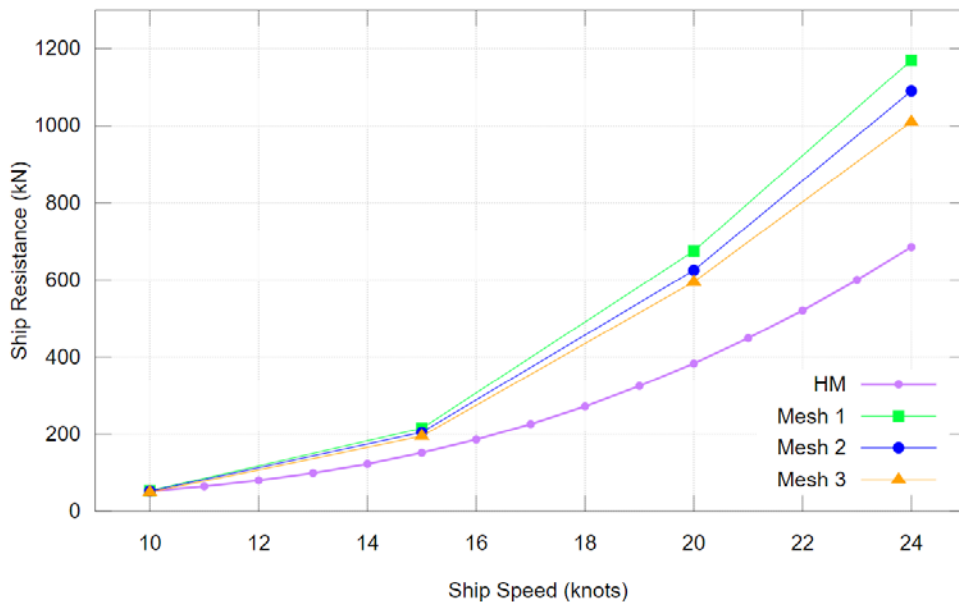

Figure 4: Ship Resistance (kN) vs Ship Speed (knots)

A comparison of results from all the meshes is shown in Table 4 for the purpose of mesh sensitivity study. It shows the variations in the results for ship resistance as a result of variation in the mesh used for simulations. The simulations with finer meshes (mesh 2 and mesh 3) give progressively lower values of ship resistance compared to the simulation with a coarse mesh (mesh 1).

The ship resistance calculated with the finest mesh, mesh 3 gives a 6.6% lower value as compared to the coarsest mesh, mesh 1 at a ship speed of 10 knots. The greatest difference between the results is at the maximum operating speed of 24 knots where mesh 3 gives a 13.7% lower value of ship resistance compared to mesh 1.

Table 4: Mesh sensitivity (difference in percentage compared to mesh 1)

Ship speed (knots)	Mesh 1 (kN)	Mesh 2 (kN)	Mesh 3 (kN)
10	53.2	52.7 (-0.9%)	49.7 (-6.6%)
15	214.5	205.4 (-4.2%)	196.1 (-8.6%)
20	677.8	636.6 (-7.6%)	593.5 (-12.4%)
24	1170.3	1097.9 (-6.2%)	1010.1 (-13.7%)

The use of free gridding and FAVOR meshing methods in Flow-3D allows us to safely conclude that the accuracy of the simulations increases as the cell size is reduced [12]. Thus, the results from the simulations using mesh 3 are the most accurate of the three simulations and the closest to the actual values of the ship resistance. The most optimal mesh is usually a trade-off between the accuracy and the time taken for the simulations.

Table 5: Ship resistance from simulations vs Holtrop-Mennen method

Ship speed (knots)	Mesh 3 (kN)	Holtrop-Mennen (kN)	Difference (%)
10	49.7	51.1	4.02
15	196.1	152.3	-22.34
20	593.5	383.6	-35.37
24	1010.1	685.4	-32.15

Table 5 shows the deviations from the simulations with mesh 3 from the calculations with the Holtrop-Mennen method. The ship resistance from both methods are similar at a ship speed of 10 knots. The difference between the results from simulations and HM method increase substantially for higher ship speeds. The greatest difference is of 35.37% at a ship speed of 20 knots. The difference comes down marginally to 32.15% at the maximum operating speed of 24 knots.

8. CONCLUSION

CFD simulations were carried out to find the ship resistance of a RoPax ferry at various ship speeds and cell sizes using Flow-3D. The results were compared to the calculations from the Holtrop-Mennen method.

The results from the simulations confirm with the HM method for lower ship speeds. As the ship speed increases, the ship resistance from the simulations are considerably higher than the calculations with the HM method.

The HM method is based on regression analysis of previous ship designs and thus some deviation from the CFD simulations should be expected. A recommendation for future work can be to analyze and compare the different components of the ship resistance from CFD simulations and the HM method. Towing tank tests were not performed due to practical limitations. It would also be interesting to use the CFD techniques discussed in this article to compare the results with a scaled model in a towing tank. This would be the only way to confirm the accuracy of the method.

Similar to the variations in the results due to different meshes, there can be variations in the results due to the choice of the turbulence model. Another suggestion for future work can be to compare these results using the traditional k-ε turbulence model to the Wilcox k-ω and the ReNormalization Group (RNG) k-ε turbulence models.

Flow-3D's capability of running ship resistance simulations has been demonstrated. The 'free gridding' and FAVOR meshing methods have proved to be time saving and hassle free as compared to other meshing techniques using body fitting meshes. This method is unique to the Flow-3D software and does not sacrifice accuracy. The software package proves to be suitable for ship hydrodynamics applications involving ship-sea interaction and other applications involving free surface flows.

The ship designers can use these results of ship resistance for hull design optimizations and for designing the propulsion system. The ship operator can use these values to evaluate an optimal operational speed for the ship considering fuel economy and other factors that might be important for the ship operator.

ACKNOWLEDGMENT

REFERENCES

[1] K. Min and S. Kang, "Study on the form factor and full-scale ship resistance prediction method," Journal of Marine Science and Technology, vol. 15, pp. 108-118, June 2010.

[2] A. Molland, S. Turnock and D. Hudson, "Ship Resistance and Propulsion" Second Edition. In Ship Resistance and Propulsion: Practical Estimation of Ship Propulsive Power (pp. 12-69), August 2017, Cambridge University Press.

[3] K. Niklas and H. Pruszko, "Full-scale CFD simulations for the determination of ship resistance as a rational, alternative method to towing tank experiments," Ocean Engineering, vol. 190, October 2019.

[4] A. Elkafas, M. Elgohary and A. Zeid, "Numerical study on the hydrodynamic drag force of a container ship model," Alexandria Engineering Journal, vol. 58, no. 3, pp. 849-859, September 2019.

[5] J. Holtrop and G. Mennen, "An approximate power prediction method," International Shipbuilding Progress, vol. 29, no. 335, pp. 166-170, July 1982.

[6] E. Bøckmann and S. Steen, "Model test and simulation of a ship with wavefoils," Applied Ocean research, vol. 57, pp. 8-18, April 2016.

[7] K. Atreyapurapu, B. Tallapragada and K. Voonna, "Simulation of a Free Surface Flow over a Container Vessel Using CFD," International Journal of Engineering Trends and Technology (IJETT), vol. 18, no. 7, pp. 334-339, December 2014.

[8] J. Petersen, D. Jacobsen and O. Winther, "Statistical modelling for ship propulsion efficiency," Journal of Marine Science and Technology, vol. 17, pp. 30-39, December 2011.

[9] H. Versteeg and W. Malalasekera, An introduction to computational fluid dynamics: the finite volume method (second edition), Harlow, England: Pearson Education Ltd, 2007.

[10] C. Hirth and B. Nichols, "Volume of fluid (VOF) method for the dynamics of free boundaries," Journal of Computational Physics, vol. 39, no. 1, pp. 201-225, January 1981.

[11] A. Nordli and H. Khawaja, "Comparison of Explicit Method of Solution for CFD Euler Problems using MATLAB® and FORTRAN 77," International Journal of Multiphysics, vol. 13, no. 2, 2019.

[12] FLOW-3D® Version 12.0 User's Manual (2018). FLOW-3D [Computer software]. Santa Fe, NM: Flow Science, Inc. https://www.flow3d.com.

[13] D. McCluskey and A. Holdø, "Optimizing the hydrocyclone for ballast water treatment using computational fluid dynamics," International Journal of Multiphysics, vol. 3, no. 3, 2009.

[14] M. Breuer, D. Lakehal and W. Rodi, "Flow around a Surface Mounted Cubical Obstacle: Comparison of Les and Rans-Results," Computation of Three-Dimensional Complex Flows. Notes on Numerical Fluid Mechanics, vol. 49, p. 1996.

[15] G. Wei, "A Fixed-Mesh Method for General Moving Objects in Fluid Flow", Modern Physics Letters B, vol. 19, no. 28, pp. 1719-1722, 2005.

[16] J. Michell, "The wave-resistance of a ship," The London, Edinburgh, and Dublin Philosophical Magazine and Journal of Science, Vols. 45, 1898, no. 272, pp. 106-123, May 2009.